JME

Journal of Mining & Environment,
Vol.8, No.3, 2017, 321-335.
DOI: 10.22044/jme.2016.628

A new stochastic 3D seismic inversion using direct sequential simulation and co-simulation in a genetic algorithm framework

H. Sabeti[1,3*], A. Moradzadeh[2], F. Doulati Ardejani[2] and A. Soares[3]

1. School of Mining, Petroleum & Geophysics Engineering, Shahrood University of Technology, Shahrood, Iran
2. School of Mining Engineering, College of Engineering, University of Tehran, Tehran, Iran
3. Petroleum Group, CERENA, Instituto Superior Tecnico, University of Lisbon, Lisbon, Portugal

Received 12 February 2016; received in revised form 11 April 2016; accepted 1 May 2016
**Corresponding author: hamid.sabeti@gmail.com (H. Sabeti).*

Abstract
Stochastic seismic inversion is a family of inversion algorithms in which the inverse solution was carried out using geostatistical simulation. In this work, a new 3D stochastic seismic inversion was developed in the MATLAB programming software. The proposed inversion algorithm is an iterative procedure that uses the principle of cross-over genetic algorithms as the global optimization technique. The model perturbation towards the objective function is performed recurring to direct sequential simulation and co-simulation. This new algorithm was applied to a synthetic dataset with and without noise. The results obtained for the inverted impedance were satisfactory in both cases. In addition, a real dataset was chosen to be applied by the algorithm. Good results were achieved regarding the real dataset. For the purpose of validation, blind well tests were done for both the synthetic and real datasets. The results obtained showed that the algorithm was able to produce inverted impedance that fairly matched the well logs. Furthermore, an uncertainty analysis was performed for both the synthetic and real datasets. The results obtained indicate that the variance of acoustic impedance is increased in areas far from the well location.

Keywords: *Seismic, Acoustic Impedance, Direct Sequential Simulation, Stochastic Seismic Inversion, Genetic Algorithm.*

1. Introduction

Stochastic models are valuable tools for hydrocarbon reservoir characterizations in both the exploration and production stages [1]. In the reservoir characterization, any knowledge of the spatial distribution of reservoir internal properties such as porosity, permeability, and lithofacies is of great importance in order to decrease the uncertainty associated with a given hydrocarbon field, and for a better decision-making [1, 2]. Over the last decade, the use of stochastic simulation algorithms has become a common industrial practice during the geo-modeling workflow, mainly due to its potential in assessing the spatial uncertainty of the property that is modeled. Among these methodologies, the most common approaches are the sequential indicator simulation for the morphological characterization of lithofluid facies [3], sequential Gaussian simulation [4], direct sequential simulation [5], and stochastic simulations conditioned to multi-point statistics [6].

In the early appraisal stage of the reservoir, the sparse core and well-log data is only available within the field of study. Although this high-resolution data provides detailed and reliable information about the reservoir properties of interest along the well path, they are limited to a few sub-surface locations. Once the internal reservoir properties are modeled, exclusively based on the available well-log data, the resulting models exhibit a great level of uncertainty, particularly at distances far from the well locations [2]. In order to get more reliable models with less uncertainty far from the wells location, it

is common to incorporate other geophysical data such as seismic reflection within the geo-modelling workflow. The seismic reflection data covers a great spatial extent at a relatively low cost but only provides an indirect measurement of the sub-surface properties of interest comparing with the well-log data. However, before incorporating this data, it is first required to solve a non-linear, ill-posed, seismic inversion problem with a multiple-solution problem [7].

The most common seismic inversion methods are categorized as deterministic. They have been used for several decades since they are less computational and easy to use. Deterministic methods allow retrieving a single inverse model of the elastic properties of interest that best fit the observed recorded seismic data. The most common methods in practical cases are the model-based and sparse-spike ones [8, 9]. These are easily implemented, and normally by a linearization around the best-fit inverse solution [10]. In spite of their widespread application, the uncertainty assessment of deterministic solutions is limited. Stochastic seismic inversion is a kind of geo-statistical inversions, where the inverse solution is achieved by sampling the model parameter space by geo-statistical sequential simulation combined with global optimization algorithms. Genetic algorithms [11-16] and simulated annealing [17, 18] are the most common techniques used within this class of inversion. Geo-statistical inversion uses sequential simulation iteratively as the model parameter perturbation technique. For each elastic model generated during a given iteration, the synthetic seismic data is computed and compared with the observed seismic data on a trace-by-trace basis. The misfit between the real and synthetic data is then used to guide the iterative procedure towards the solution.

The first geo-statistical seismic inversion methods were introduced by Bortoli et al. (1992) [19] and Haas and Dubrule (1994) [20]. In their sequential trace-by-trace approach, each seismic trace was visited individually following a pre-defined random path that visits all the gridding locations. At each step along the random path, a set of numerous acoustic impedance (AI) traces was simulated using Sequential Gaussian Simulation (SGS). Then for each individual simulated impedance trace, the corresponding reflection coefficient was derived and convolved by a wavelet. It resulted in a set of numerous synthetic seismic traces, which was individually compared, in terms of the correlation coefficient, against the recorded seismic trace. The acoustic impedance model that produced the highest correlation coefficient between the real and synthetic seismic traces was stored in the reservoir grid and considered as the conditioning data for simulation of a new set of acoustic impedance models at the new location considered in the pre-defined random path [19, 20]. Note that for the first location along the random path, the acoustic impedance models were simulated exclusively conditioned to the available acoustic impedance log data. The following locations were conditioned not only to the available experimental data but also by the acoustic impedance traces already simulated in the previous steps. The inversion process was finished after all the trace locations were visited. Since the random path changed on each individual geo-statistical inversion run, and consequently, modified the conditioning data at each trace location, different runs produced variable inverted acoustic impedance models that fitted equally the observed seismic reflection data. All the possible solutions were achieved under the same assumptions regarding the global probability distribution function and spatial continuity model as retrieved from the experimental data, i.e. the available well-log dataset.

Afterwards, Soares et al. (2007) [5] introduced the global stochastic inversion methodology. Contrary to the trace-by-trace approaches [19, 20], they proposed a global approach during the stochastic simulation stage. This family of algorithms was iterative procedures that used the principle of cross-over genetic algorithms as the global optimization technique and where the model perturbation towards the objective function was performed recurring to direct sequential simulation and co-simulation [14, 21, 22]. The procedure generated, at once and for the entire seismic grid, a set of impedance models. Each impedance model was then convolved to create a set of synthetic seismic volumes, which were compared with the recorded seismic cube. Although this method is computationally expensive, it allows a more comprehensive exploration of model space since more simulation models have been performed for the inversion. In the conventional algorithm [14], the correlation coefficient between the synthetic and real recorded seismic traces was done for the entire vertical samples of each trace. This is the easiest way, and probably less computational. However, it is possible to make a random layering map in which a partial vertical set of samples is selected

to be compared regarding the synthetic and recorded seismic data. In this work, a new implementation of the stochastic seismic inversion was developed in the MATLAB programming software. In this new algorithm, a comparison is made between the synthetic and real seismic traces using a layering map, where the random parts of a trace are selected to calculate the correlation coefficient. In addition, an earlier work [14] introduced the inversion method very briefly and did not present comprehensive results and blind well tests. In the current work, however, the new code was applied and investigated deeply on both the synthetic and real datasets. Since this algorithm is the only one that performs the inversion in a global condition, blind-well tests were used to validate the method for both the synthetic and real datasets.

2. Direct sequential simulation and co-simulation

The Direct Sequential Simulation (DSS) algorithm was initially proposed by Soares (2001) [5]. This algorithm uses a global probability distribution and a spatial continuity pattern when simulating a studied area. In comparing with other sequential simulation algorithms, DSS has the advantage of using the original data domain without the need for any parametric transform, e.g. Gaussian transform. DSS generates a simulated value using the simple kriging estimate and variance, calculated within a searching neighbor based on a variogram model. Sampling is done directly using the global conditional distribution function estimated from the experimental data [5]. The simulated value at location x_u is drawn from an auxiliary probability distribution function ($F_z'(z)$), which is built from the global cumulative distribution function (CDF) $F_z(z)$. $F_z'(z)$ is defined by selecting an interval over $F_z(z)$ centered on the simple kriging estimate ($z(x_u)^*$) (Equation 1), the value with an interval range proportional to the kriging variance, σ_{sk}^2 (Equation 2).

$$\frac{1}{n}\sum_{i=1}^{n} z(x_i) = z(x_u)^* \quad (1)$$

$$\frac{1}{n}\sum_{i=1}^{n} [z(x_i) - z(x_u)^*]^2 = \sigma_{sk}^2(x_u) \quad (2)$$

One way of constructing $F_z'(z)$ is by defining a local Gaussian CDF, $G(y(x_u)^*, \sigma_{sk}^2(x_u))$, created by the Gaussian transform of the interval of $F_z(z)$ centered in $z(x_u)^*$ (Equation 1) with an amplitude proportional to σ_{sk}^2 (Equation 2).

The DSS simulation algorithm can be summarized in the following sequence of steps [5]:

1) Generate a random seed to define a random path over the entire simulation grid $x_u, \mathrm{u} = 1, \dots, N$, where *N* is the total number of nodes that compose the simulation grid;

2) Estimate the local mean, $\mathrm{z}(x_u)^*$, and variance, $\sigma_{\mathrm{sk}}^2(x_u)$, with simple kriging estimate conditioned to the original experimental data and previously simulated data, within a neighborhood around **u**;

3) Define the interval $\mathrm{F_z(z)}$ to be sampled, as previously explained;

4) Draw the $\mathrm{z^s}(x_u)$ value from CDF of $\mathrm{F_z(z)}$;

- Generate the u value from the uniform distribution between [0, 1]
- Generate the $\mathrm{y^s}$ value from $\mathrm{G(y}(x_u)^*, \sigma_{\mathrm{sk}}^2(x_u))$
- Return the simulated value $\mathrm{z^s}(x_u) = \varphi^{-1}(\mathrm{y^s})$

5) Loop until all the N nodes of the simulated grid have been simulated.

3. A new stochastic seismic inversion in a genetic algorithm framework

Stochastic seismic inversion is a type of geo-statistical inversion methods, in which spatial continuity is taken into account for deriving acoustic impedance models from seismic data. Soares et al. (2007) [14] proposed a stochastic inversion algorithm, and briefly presented a case study. In their algorithm, the comparison between the total real and synthetic traces was used as the objective function of a genetic algorithm. Using an entire trace for calculating the correlation coefficient inside the inversion procedure made it difficult for the iterative process to be converged since the simulated values of impedance may vary a lot due to the geo-statistical simulation nature. In our new algorithm, a modification is proposed inside the inversion procedure that compares a partial trace selection to calculate the correlation coefficient between the real and synthetic seismic data. The partial selection of a trace is defined by a "layering" map in which the number of vertical grid number of each part of the trace is generated randomly. At the beginning of each iteration, a new layering map is generated randomly to avoid any discontinuity artifact. The flowchart of the proposed inversion method is briefly described by Figure 1. First a user-defined number (e.g. *N*) of acoustic impedance cubes is generated using the direct sequential simulation algorithm.

Convolving a seismic wavelet, we are able to create *N* cubes of synthetic seismic. In this step, instead of calculating the correlation coefficients between each trace of the cube, a random division of all cubes is done first. Notice that the division is random but the same for all cubes in each iteration in order to make it possible to calculate the correlation coefficients in a regular grid. Now each part of each trace in *N* cubes is extracted and compared with the corresponding part from the real seismic, leading to a correlation coefficient value. Then all *N* cubes are merged into a single cube by selecting the best parts of acoustic impedance values. "Best part" means that acoustic impedance values correspond to the higher correlation coefficient values of all N cubes. In this step, a cube of the highest correlation coefficient values related to each part is also created. The first iteration is finished here, and the algorithm is ready to do the next iteration, which is quite different. The second iteration is begun by simulating *N* new cubes of acoustic impedance using direct sequential co-simulation. The well logs, "best parts" cube of acoustic impedance, and cube of highest correlation coefficients from the previous iteration are used to do the co-simulation of *N* acoustic impedance cubes. Then the corresponding synthetic seismic cubes are generated, and a set of new correlation coefficients is calculated using a new layering map. A new "best parts" cube of acoustic impedance and a new cube of highest correlation coefficients are created. The algorithm proceeds until the total number, if iteration is achieved. In the last iteration, there are *N* numbers of acoustic impedance cubes in which the highest correlation coefficient values are obtained. The entire procedure does the optimization based on a genetic algorithm. Genetic algorithm is the name given to a process which relies on producing different generations, each created using the previous one, and evaluated through an objective function. The proposed algorithm is called genetic because there are "generations" (iterations) with several "individuals" (simulations). For each generation, the best parts of the individuals are used to reproduce the next generation, and the worse parts are just ignored. The objective function is the mismatch between the synthetic and real seismic data using the Pearson correlation coefficient formula.

4. Application of new inversion algorithm to a synthetic dataset

The synthetic dataset used for this research work consisted of the 3D seismic data and acoustic impedance logs of 14 wells. The inversion gridding dimension was 101×101×90. Figure 2a shows a 3D view of the well locations in the gridding cube. Two wells were excluded from the inversion process to be used for blind-well tests (Figure 2b). The seismic wavelet used to create the seismic data is shown in Figure 3. The first step of the geo-statistical inversion was variogram modeling. Both the horizontal and vertical variogram models were calculated using the impedance logs of the wells (Figure 4). The algorithm was then applied using the variogram models. There were 64 realizations per iteration to explore the model space. After 6 iterations, a satisfactory convergence was achieved. Figure 5a presents a vertical section of the input seismic data crossing one of the wells. Figure 5b shows the best inverted impedance model of the algorithm. Figure 5c illustrates the corresponding synthetic seismic section that has been resulted by convolution of seismic wavelet (Figure 3) with the calculated reflection coefficient (RC) series. As it can be seen in Figure 5c, all reflectors were reproduced in the synthetic seismic section with more additional details.

In order to evaluate the ability of the proposed algorithm in inversion of noise-contaminated data, a randomly noise-added seismic cube was generated with a signal to noise ratio of 4 dB. After adding noise, weak reflectors on top of the section were intensively destroyed, while sharp reflectors lost their continuity, especially in the bottom area (Figure 6a). The inverted impedance model is shown in Figure 6b. Figure 6c presents the synthetic seismic section. In this figure, most sharp reflectors were reproduced after inversion. However, there are some areas in which some reflectors were not reproduced properly, probably due to the intense level of noise compared to the seismic signal.

The global correlation coefficient between the real (input) and synthetic (inverted) seismic data for the noise-free and noisy datasets were 0.76 and 0.71, respectively. Figure 7 shows the convergence revolution for both the noise-free and noisy data.

Any stochastic inversion method must respect the mean and variance of the hard data (well logs) in the final inverted model of the property of interest. Table 1 compares these parameters. As expected, both the mean and variance values were properly reproduced in the inverted acoustic impedance model. It can be seen that the variance

for the inverted impedance of noisy dataset is high. This is caused by the high level of noise, where seismic signals were damaged. In this situation, the algorithm simulates higher range impedance values. Consequently, the variance becomes high. In addition, the histogram of the impedance data for both the well logs and inverted models are presented in Figure 8. In this figure, the histogram reproduction can be seen in the inverted impedance model for both the noise-free and noisy datasets. In case of the noise-free dataset, the impedance histogram is reproduced perfectly, while there is a slight difference in the impedance histogram of the noisy dataset. Nevertheless, the main populations were reproduced (Figure 8c).

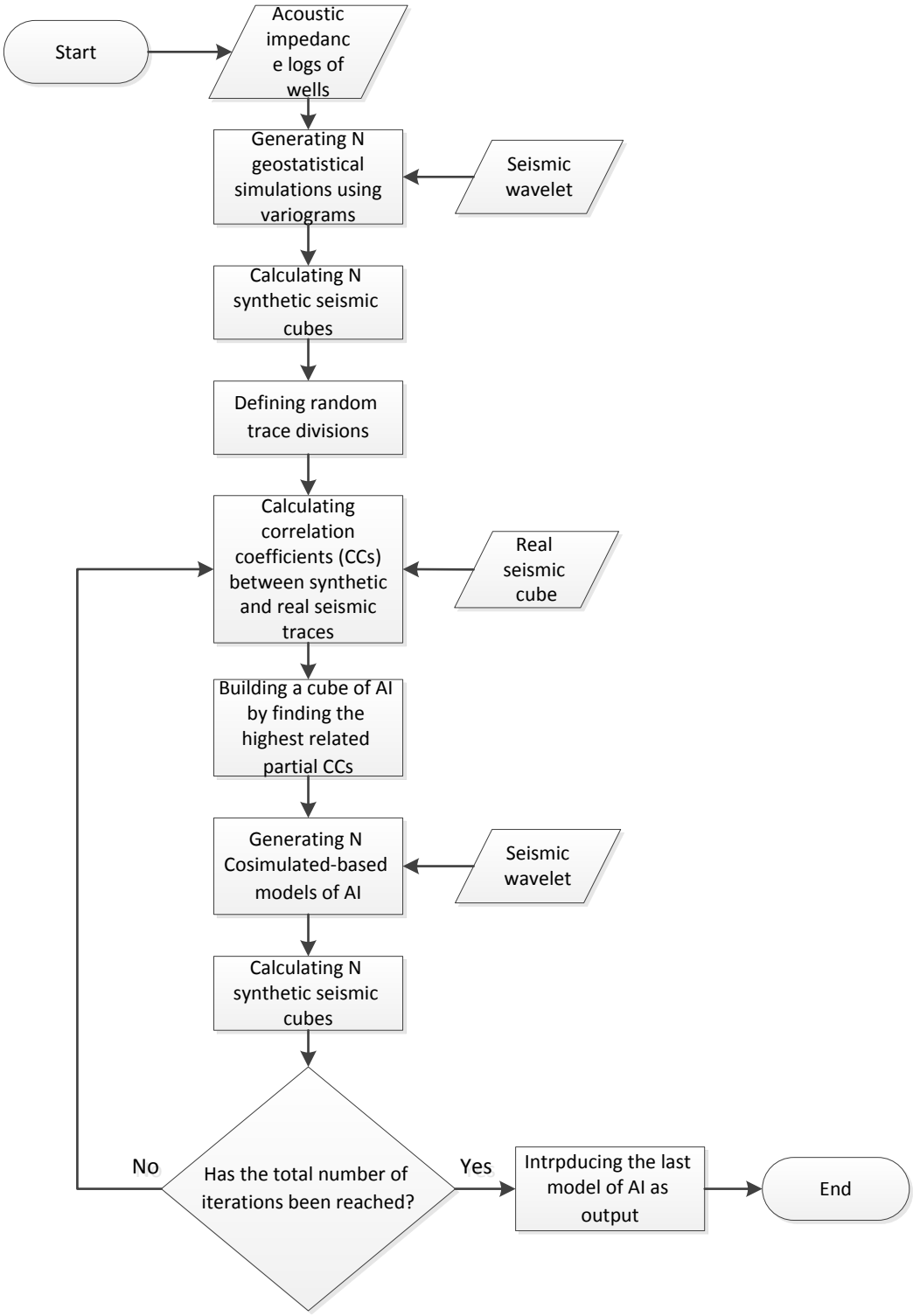

Figure 1. Flowchart of proposed stochastic seismic inversion algorithm.

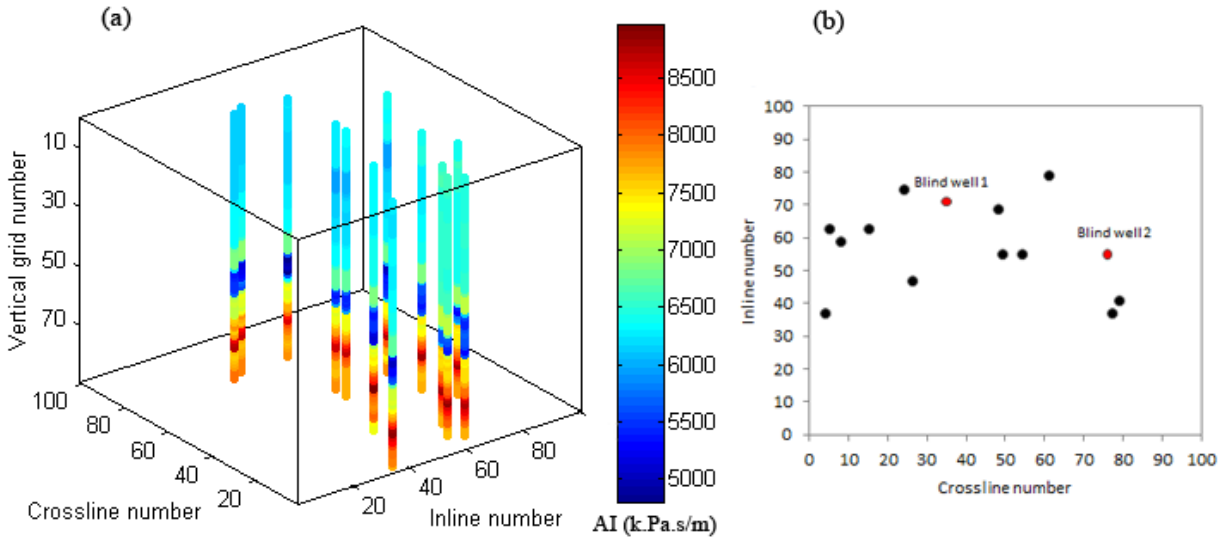

Figure 2. a) 3D view of inversion gridding and well locations, b) 2D well locations of synthetic dataset.

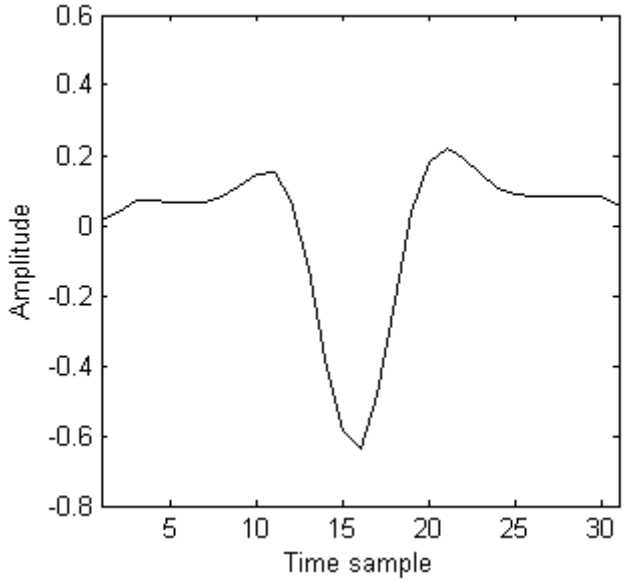

Figure 3. Seismic wavelet used for synthetic dataset.

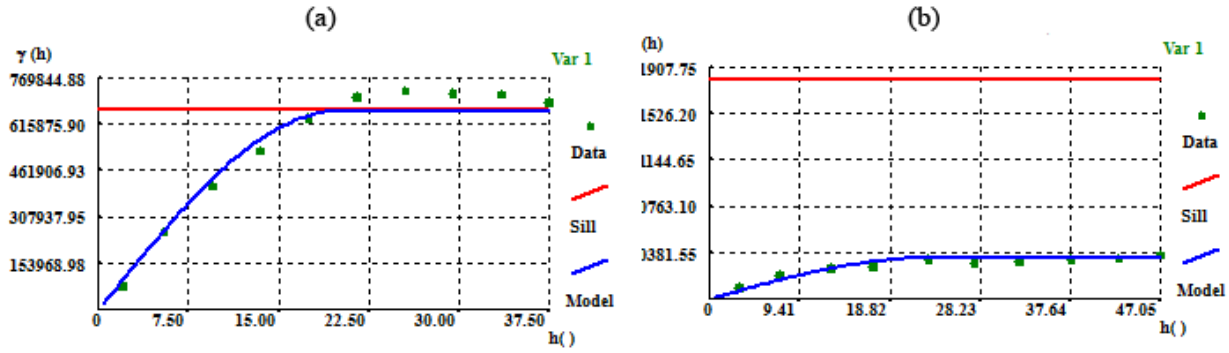

Figure 4. Variogram models of impedance logs of synthetic dataset: a) vertically, b) horizontally.

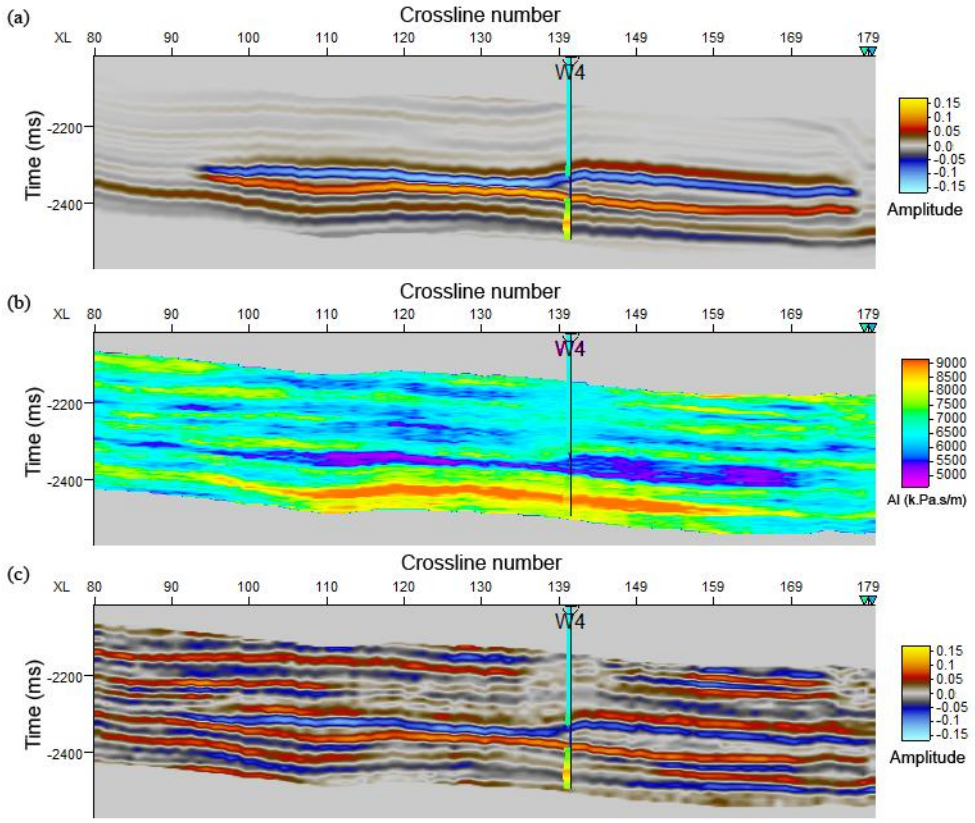

Figure 5. a) A vertical section of input seismic data, b) inverted impedance model, and c) synthetic seismic section after convolution with seismic wavelet (Figure 3).

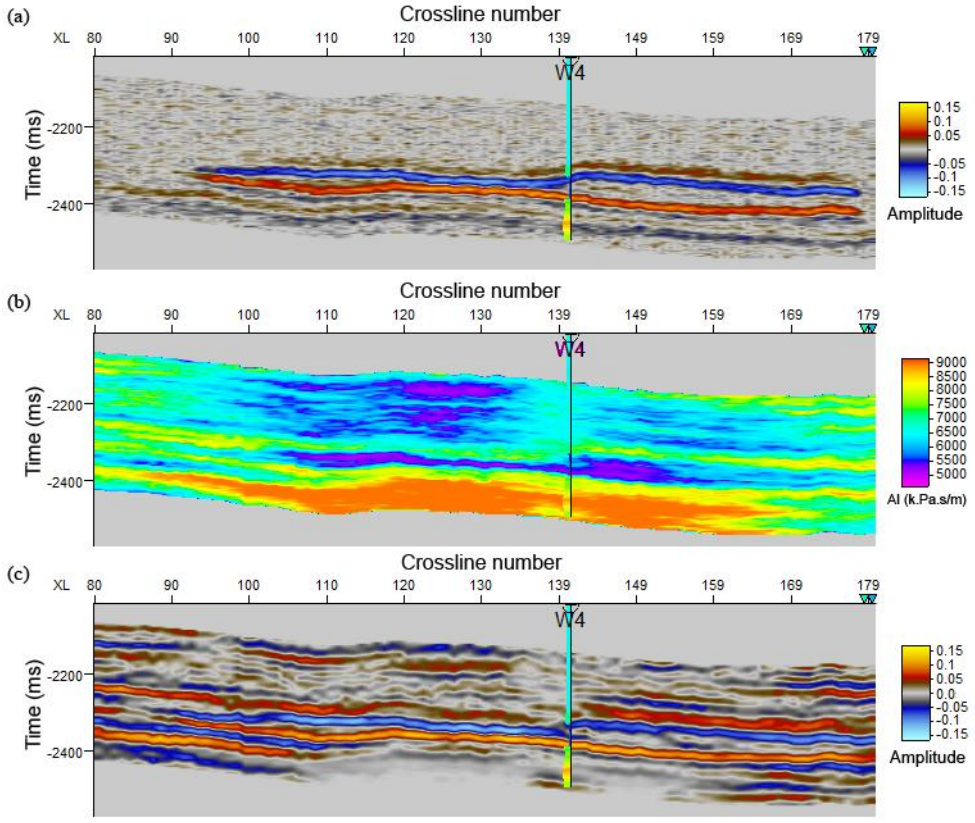

Figure 6. a) A vertical section of input noisy seismic data, b) inverted impedance model, and c) synthetic seismic section after convolution with seismic wavelet (Figure 3).

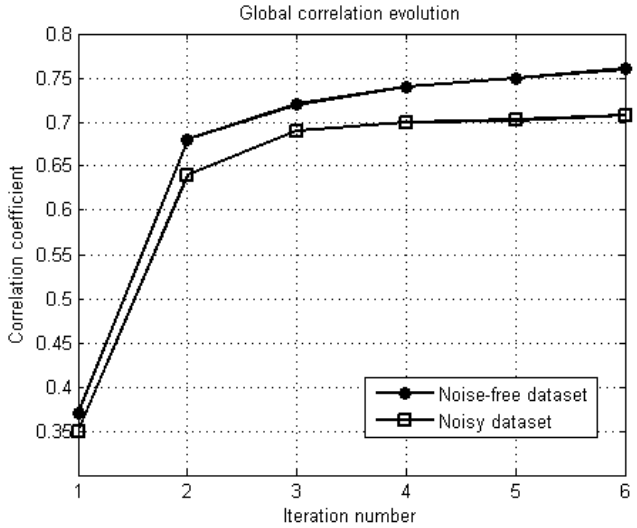

Figure 7. Convergence of algorithm for both noise-free and noisy synthetic datasets. Correlation coefficient values are between real (input) and synthetic (inverted) seismic data.

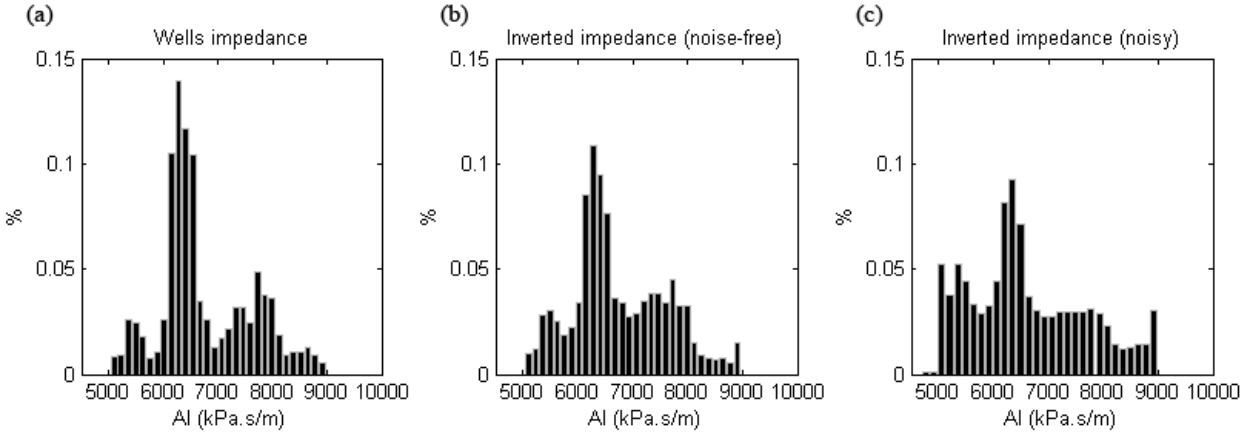

Figure 8. Acoustic impedance histograms for a) well logs, b) inverted model of noise-free dataset, and c) inverted model of noisy dataset.

Table1. Mean and variance of acoustic impedance values.

	Mean (k.Pa.s/m)	Variance (k.Pa.s/m)^2
Acoustic impedance of well logs	6750	702692
Inverted acoustic impedance (noise-free)	6664	717666
Inverted acoustic impedance (noisy)	6612	934767

4.1. Blind-well test for synthetic dataset

Two wells were excluded from the inversion process to do the blind-well tests (Figure 2b). The acoustic impedance logs of these two wells were upscaled into inversion gridding in order to be comparable with the inverted acoustic impedance of the same spatial locations. Table 2 presents the correlation coefficients between the well logs and the inverted acoustic impedance for the two blind wells. In addition, Figure 9 shows the impedance plots of well logs, and the inverted impedance of noise-free and noisy datasets for both blind wells. There are good matches between the impedance logs and the inverted impedance in case of the noise-free dataset for both blind wells. However, for the noise-contaminated dataset, there are some variations in the inverted impedance values, which are mainly due to artifacts caused by the noisy seismic data.

Table 2. Correlation coefficients between impedance well logs and inverted models.

	Noise-free dataset	Noisy dataset
Blind well 1	93%	83%
Blind well 2	87%	56%

4.2. Uncertainty analysis for synthetic dataset

One of the main advantages of the stochastic inversion methods versus the deterministic ones is the possibility of producing various outputs named as realizations. All these realizations are conditioned to the well logs and seismic data. This makes it possible to generate a variance cube using all impedance models of the last iteration. Figure 10a shows the vertical section of the variance model related to the noise-free synthetic dataset. As expected, the areas close to the well have a lower variance, meaning less uncertainty. Variance normally increases where we are distancing from the well. This is not a general rule since there may be other reasons for increasing the variance far from a well. Increasing the variance might be caused by weak seismic signals or low correlation between the well logs and seismic data. The latter reason sometimes spreads over the inversion gridding since the simulated values come from neighboring values using a variogram model. Figure 10b represents the same vertical section related to the noisy dataset. As expected, the variance values were raised due to the significant level of noise added to the seismic data.

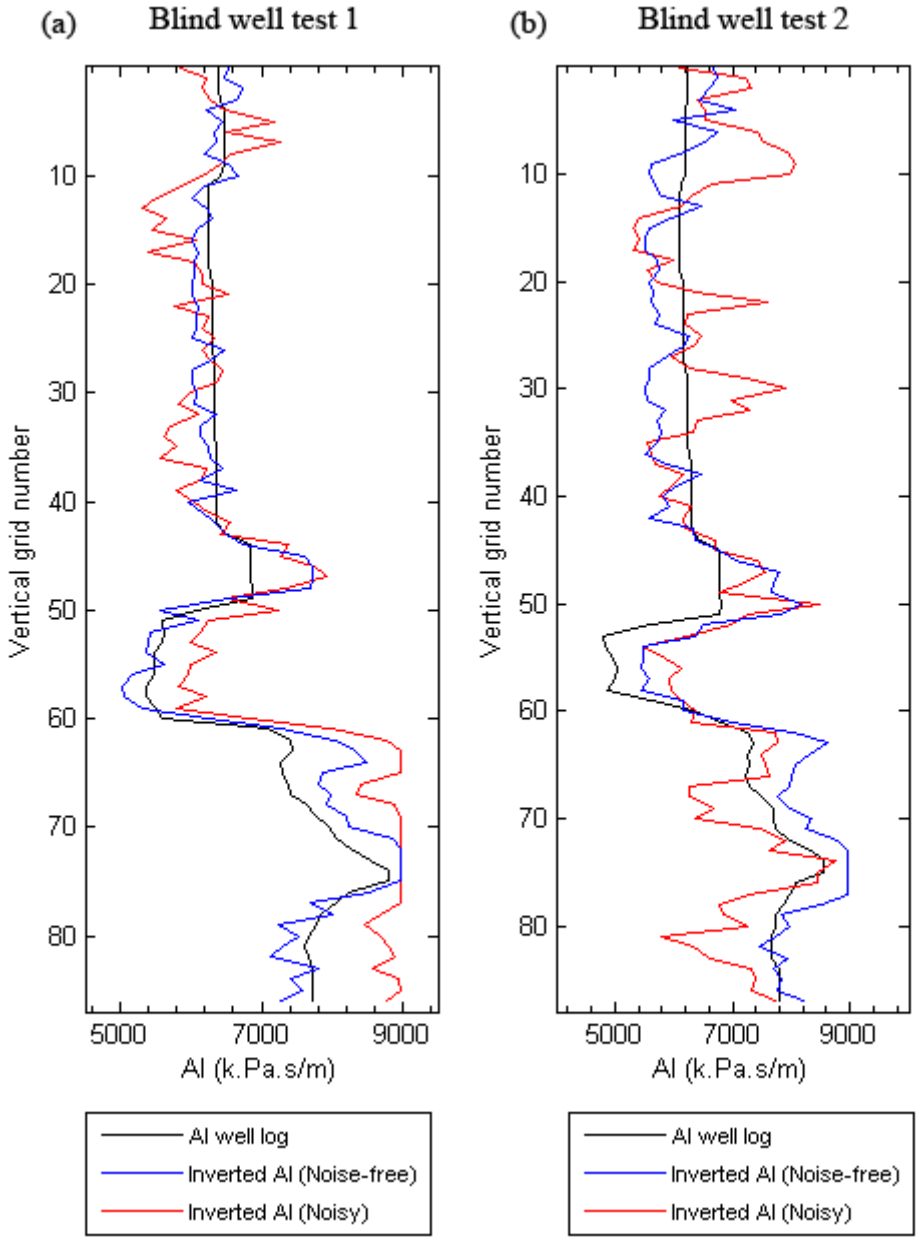

Figure 9. Blind-well tests for synthetic dataset. Plots of acoustic impedance values for a) blind well 1 and b) blind well 2.

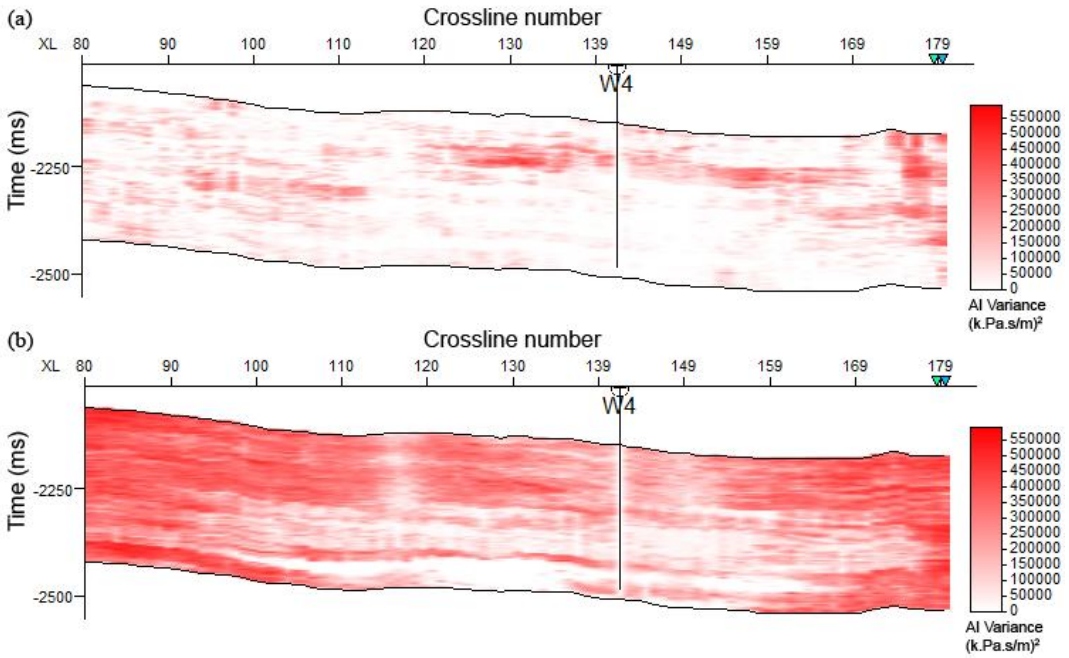

Figure 10. Vertical sections of variance model related to a) noise-free dataset and b) noisy dataset.

5. Application of proposed inversion algorithm to a real dataset

A real dataset from North Sea was chosen to further examine the ability of the inversion algorithm. The location of the studied area is shown in Figure 11. This dataset consists of the 3D seismic and acoustic impedance data of two wells. Figure 12 shows a 3D view of inversion gridding including wells locations.

Figure 11. Map of real case study in North Sea.

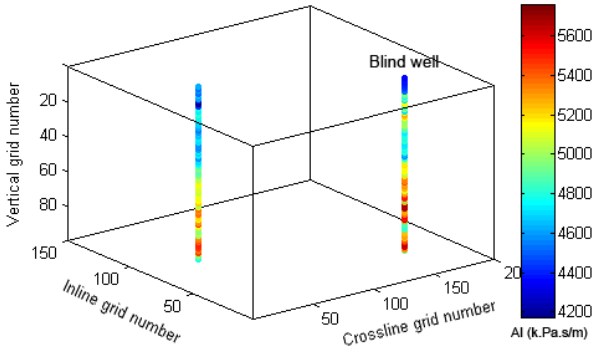

Figure 12. 3D view of inversion gridding and well locations of real dataset.

5.1. Wavelet extraction

Accurate wavelet estimation is absolutely critical to the success of any seismic inversion. The shape of the extracted wavelet (frequency and phase content) may strongly influence the inversion results, and thus the subsequent assessment of the reservoir quality. In the inversion techniques, it is assumed that the seismic data can be modeled as a convolution of the seismic wavelet with a band-limited reflection coefficient series. Wavelet estimation is conducted by computing a filter that best shapes the well-log reflection coefficients to the input seismic at the well locations. The phase of the seismic data, which may vary with frequency, is obtained by this filter. The algorithm minimizes the misfit between the seismic data and the convolution between the estimated wavelet and the reflection coefficients. The algorithm iteratively adjusts the amplitude and phase spectrum of the wavelet. In this approach, a wavelet was extracted in a way that it optimally matched both wells simultaneously. Figure 13 shows the extracted wavelet and its frequency spectrum.

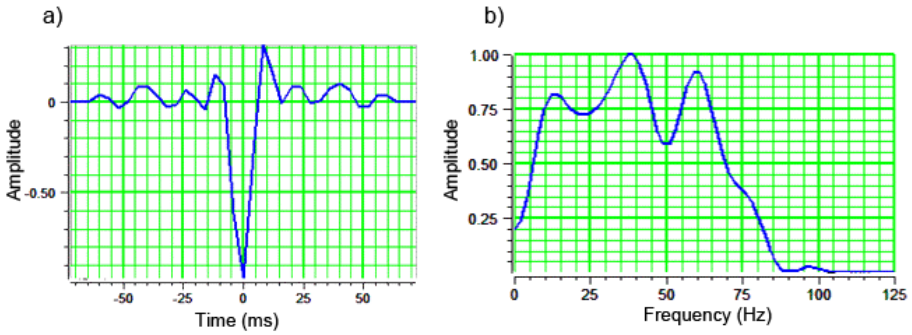

Figure 13. a) Seismic wavelet extracted for real dataset in time domain, b) frequency spectrum of wavelet.

5.2. Inversion

As shown in Figure 12, the acoustic impedance log of one well was used for inversion, and the other well was used for evaluation and validation of the inversion results. Vertical variogram modeling was completed by acoustic impedance well log. Horizontal variogram modeling was done using the seismic data. Figure 14 shows the results of variogram modeling. These variogram models were used as input for the stochastic inversion algorithm. The proposed stochastic inversion was done using 6 iterations and 64 simulations per iteration. The global correlation coefficient between the synthetic and recorded seismic data was 0.61. Figure 15 illustrates three sections, crossing the well, of real seismic data, inverted impedance, and synthetic seismic data. The inverted impedance (Figure 15b) clearly follows the seismic reflectors in Figure 15a. After convolution with the seismic wavelet (Figure 13), a synthetic seismic section was generated in Figure 15c. This synthetic seismic section has more detailed reflectors compared to the real one. The histograms of well log and inverted acoustic impedance are shown in Figure 16, proving that the histogram reproduction was successful during the proposed stochastic seismic inversion. Table 3 shows the mean and variance of well-log impedance and the final inverted model. Both these parameters were successfully reproduced by the 3D inversion of the seismic data.

Table 3. Mean and variance of acoustic impedance values.

	Mean (k.Pa.s/m)	Variance (k.Pa.s/m)^2
Well log acoustic impedance	4988	1.081×10^5
Inverted acoustic impedance	4908	1.049×10^5

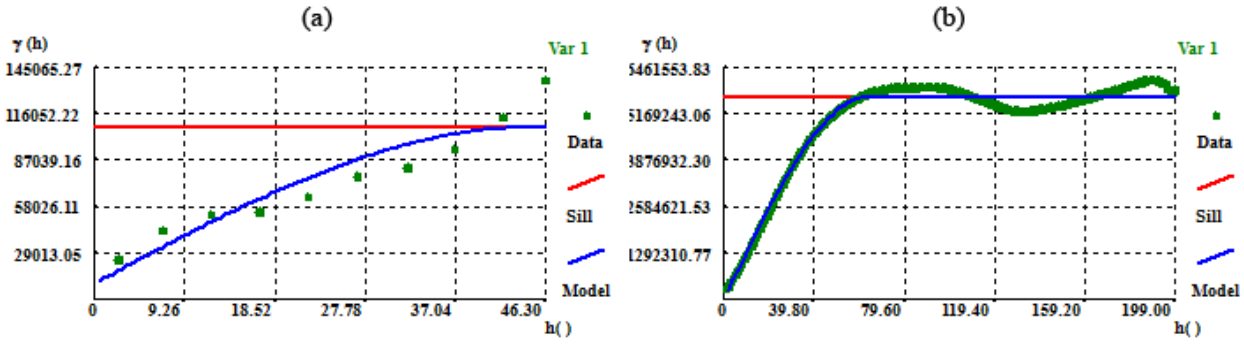

Figure 14. Variogram models of real dataset: a) vertical variogram using impedance well log, b) horizontal variogram using seismic data.

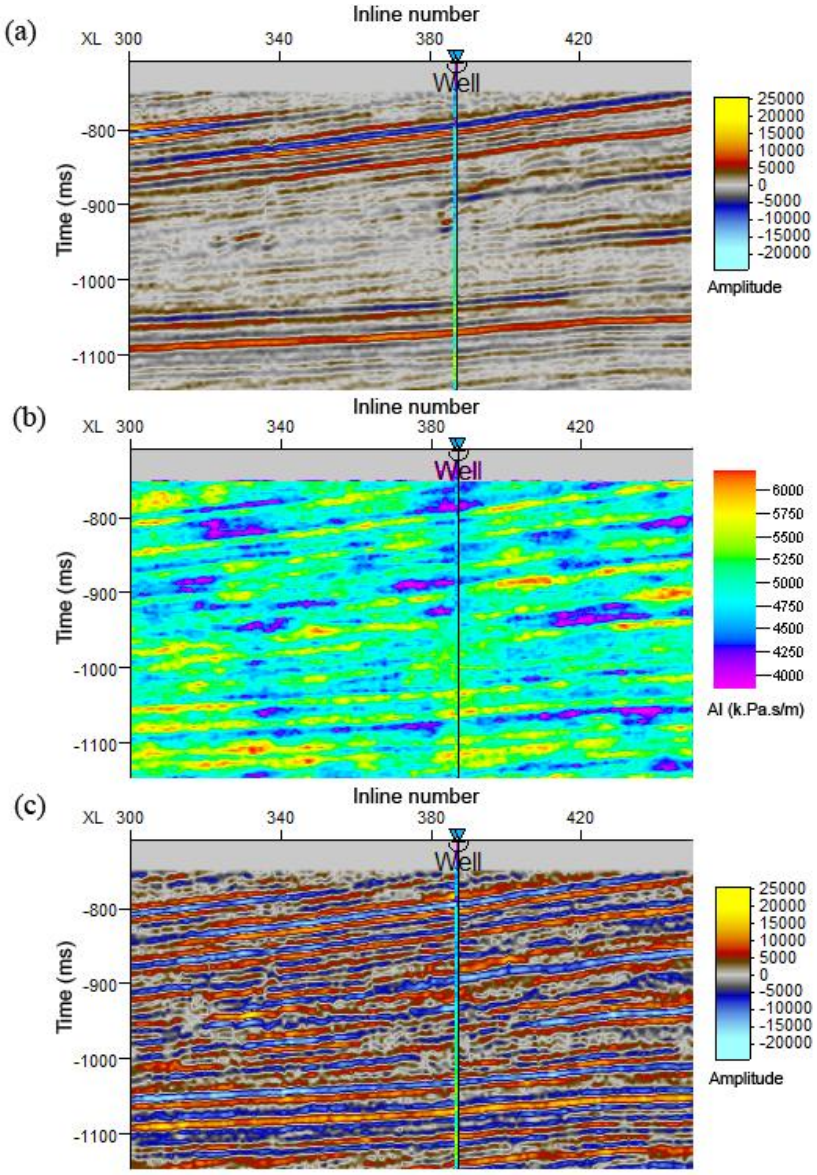

Figure 15. a) A vertical section of real seismic data, b) Inverted impedance model, c) synthetic seismic section after convolution with seismic wavelet (Figure 13).

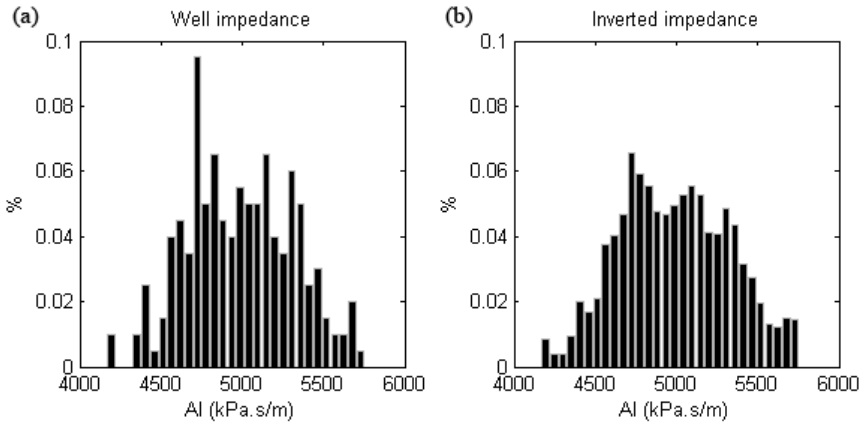

Figure 16. Acoustic impedance histograms for a) well log and b) inverted model of real dataset.

5.3. Blind well test for real dataset

One excluded well log (Figure 12) was upscaled and compared to the inverted acoustic impedance in the same location. The correlation coefficient of 0.65 between the blind-well log and the inverted acoustic impedance was achieved. Figure 17 shows two plots regarding the well-log acoustic impedance and the inverted one. Although there are some differences between the well log and the inverted values, the general trend of the well log is followed by the inverted values. Since the inversion was done using only one well, this correlation might be acceptable.

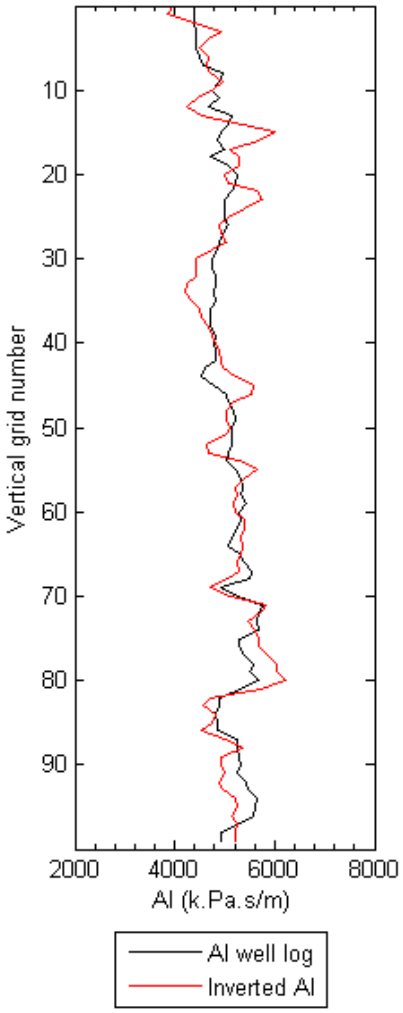

Figure 17. Blind-well test for real dataset. Impedance values of well log and inverted impedance are plotted.

5.4. Uncertainty analysis for real dataset

Using 64 simulation realizations of the last iteration, the variance was calculated over the whole 3D inversion gridding. Figure 18 shows a vertical section of the variance model crossing the well. Since the inversion was done in three dimensions, a horizontal slice of the variance is shown in Figure 19. The variance values increase the area far from the well. This is an important factor that proves the reliability of the algorithm since the simulation procedure must always honor the well-log values during the inversion. In the area far from the well, the simulation algorithm tries to generate the impedance values using a variogram model. This will normally lead to an increase in the variance.

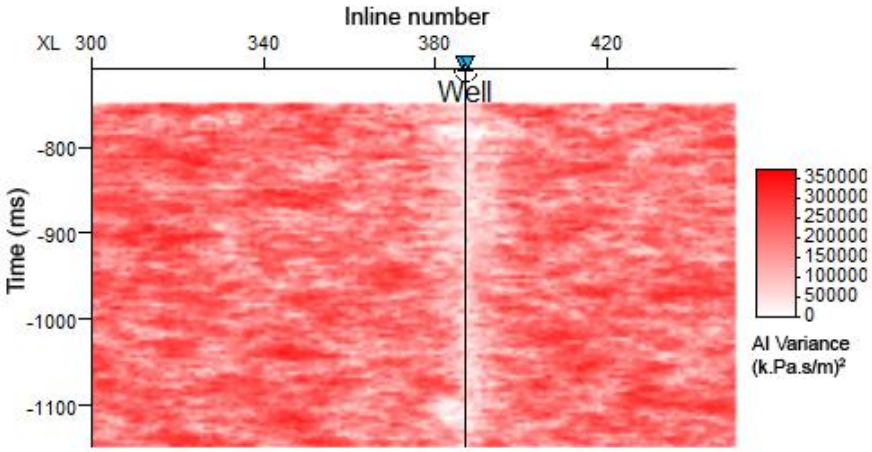

Figure 18. Vertical section of variance model crossing well related to real dataset.

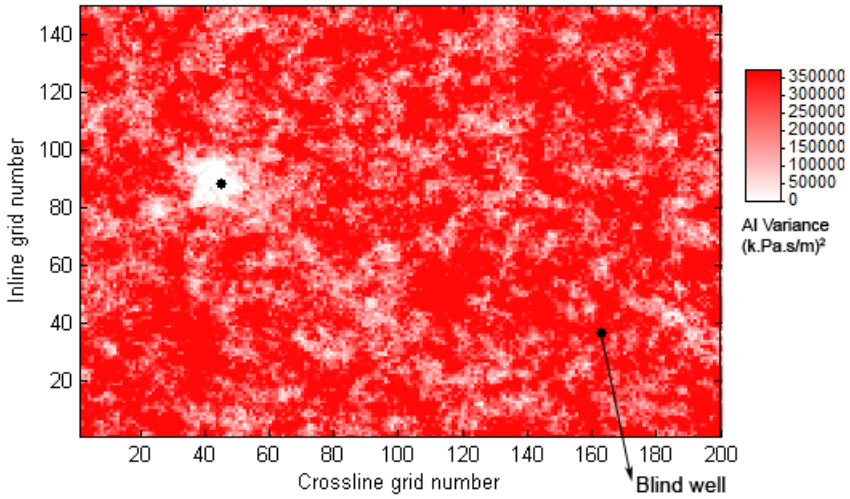

Figure 19. Horizontal slice of variance model related to real dataset. Locations of wells are presented by filled circles.

6. Conclusions

In this work, a new 3D stochastic seismic inversion was proposed using direct sequential simulation and co-simulation, and applied to both the synthetic and real datasets. The new algorithm follows a genetic framework since it has several generations (iterations) with several individuals (simulations). Application to a synthetic dataset, with and without noise, showed that the proposed algorithm is able to properly invert the seismic data into acoustic impedance models. The comparisons of acoustic impedance logs of two blind wells with those of the inverted impedance indicate a good correlation value. This correlation, of course, decreased in the case of using noisy data. It was also shown that histograms, mean, and variance of the well logs were reproduced in the final inverted impedance model for all cases. Moreover, application of the proposed inversion procedure to a real dataset revealed that the algorithm was successful in producing the inverted impedance models. Blind-well test for a real dataset showed an acceptable correlation

between the well log and the inverted impedance values.

The proposed algorithm has the ability of producing several inverted models, all of which honor the input data. This advantage made it possible to do a kind of uncertainty analysis by calculation of the acoustic impedance variance over all the inverted models. The results of uncertainty analysis for both the synthetic and real datasets showed that the variance values of acoustic impedance generally increased where getting further from a well. This phenomenon proved that the algorithm honored the well logs during the inversion process.

References

[1]. Doyen, P.M. (2007). Seismic reservoir characterization: an earth modelling perspective. EAGE. Houten, 255 P.

[2]. Caers, J. (2011). Modeling Uncertainty in Earth Sciences. Wiley-Blackwell. New Jersey. 246 P.

[3]. Soares, A. (1998). Sequential Indicator Simulation with Correction for Local Probabilities. Mathematical Geology. 30: 761-765.

[4]. Deutsch, C.V. and Journel, A.G. (1998). GSLIB: Geostatistical software library and user's guide: Oxford Univ Press. New York. 340 P.

[5]. Soares, A. (2001). Direct Sequential Simulation and co-simulation. Mathematical Geology. 33: 911-926.

[6]. Strebelle, S. (2002). Conditional Simulation of Complex Geological Structures Using Multiple-Point Statistics. Mathematical Geology. 34 (1): 1-21.

[7]. Tarantola, A. (2005). Inverse problem theory and methods for model parameter estimation. Society for Industrial and Applied Mathematics. Pennsylvania. 342 P.

[8]. Russell, B. (1988). Introduction to seismic inversion methods. Society of Exploration Geophysicists. Oklahoma. 90 P.

[9]. Bosch, M., Mukerji, T. and González, E.F. (2010). Seismic Inversion for Reservoir Properties Combining Statistical Rock Physics and Geostatistics: A Review, Geophysics. 75 (5): 75A165-75A176.

[10]. Azevedo, L., Nunes, R., Correia, P., Soares, A., Guerreiro, L. and Neto, G. (2014). Multidimensional scaling for the evaluation of a geostatistical seismic elastic inversion methodology. Geophysics. 79: M1-M10.

[11]. Mallick, S. (1995). Model based inversion of amplitude variations with offset data using a genetic algorithm. Geophysics. 60: 939-954.

[12]. Mallick, S. (1999). Some practical aspects of prestack waveform inversion using a genetic algorithm: An example from the east Texas Woodbine gas sand. Geophysics. 64: 326-336.

[13]. Boschetti, F., Dentith, M.C. and List, R.D. (1996). Inversion of Seismic Refraction Data Using Genetic Algorithms, Geophysics. 61: 1715-1727.

[14]. Soares, A., Diet, J.D. and Guerreiro, L. (2007). Stochastic Inversion with a Global Perturbation Method, Proc., Petroleum Geostatistics, EAGE, Cascais. Portugal. September. 10-14.

[15]. Azevedo, L., Nunes, R., Soares, A., Mundin, E.C. and Neto, G.S. (2015). Integration of well data into geostatistical seismic amplitude variation with angle inversion for facies estimation. Geophysics. 80: M113-M128.

[16]. Carmo, S., Azevedo, L. and Soares, A. (2015). Seismic inversion for non-stationarity environments: a methodology benchmark, Proc., SEG 85th Annual Meeting, New Orleans, Louisiana. 18-23 October. pp. 2738-2742.

[17]. Sen, M. and Stoffa, P. (1991). Nonlinear one dimensional seismic waveform inversion using simulated annealing. Geophysics. 56: 1624-1638.

[18]. Ma, X. (2002). Simultaneous inversion of prestack seismic data for rock properties using simulated annealing. Geophysics. 67: 1877-1885.

[19]. Bortoli, L.J., Alabert, F., Haas, A. and Journel, A.G. (1992). Constraining Stochastic Images to Seismic Data, Geostatistics Troia, 1: 325-338.

[20]. Haas, A. and Dubrule, O. (1994). Geostatistical Inversion- A sequential Method for Stochastic Reservoir Modeling Constrained by Seismic Data. First Break. 12: 561-569.

[21]. Nunes, R., Soares, A., Schwedersky, G., Dillon, L., Guerreiro, L., Caetano, H., Maciel, C. and Leon, F. (2012). Geostatistical Inversion of Prestack Seismic Data, Proc., 9th International Geostatistics Congress, Oslo. 11-15 June, pp. 1-8.

[22]. Azevedo, L., Nunes, R., Soares, A. and Neto, G.S. (2013). Stochastic Seismic AVO Inversion, 75th EAGE Conference and Exhibition. London. 10-13 June.

روشی جدید برای وارون‌سازی تصادفی لرزه‌ای سه‌بعدی با استفاده از شبیه‌سازی متوالی مستقیم و شبیه‌سازی توامان در چهارچوب الگوریتم ژنتیک

حمید ثابتی[۳،۱*]، علی مراد زاده[۲]، فرامرز دولتی اردجانی[۲] و آمیلکار سوارس[۳]

۱- دانشکده مهندسی معدن، نفت و ژئوفیزیک، دانشگاه صنعتی شاهرود، ایران

۲- دانشکده فنی و مهندسی، دانشکده معدن، دانشگاه تهران، ایران

۳- بخش نفت، انستیتو فنی عالی، دانشگاه لیسبون، لیسبون، پرتغال

ارسال ۲۰۱۶/۲/۱۲، پذیرش ۲۰۱۶/۵/۱

* نویسنده مسئول مکاتبات: hamid.sabeti@gmail.com

چکیده:

روش‌های وارون‌سازی تصادفی شامل روش‌هایی هستند که در آن‌ها حل مسئله وارون بر اساس الگوریتم‌های شبیه‌سازی زمین‌آماری انجام می‌شود. در این پژوهش، یک روش جدید وارون‌سازی تصادفی لرزه‌ای سه‌بعدی در محیط برنامه‌نویسی MATLAB توسعه داده شده است. الگوریتم وارون سازی پیشنهادی روشی بر مبنی تکرار محاسبات است که از الگوریتم بهینه‌سازی ژنتیک برای همگرایی حل مسئله وارون استفاده می‌کند. به منظور جستجوی فضای پارامتری، الگوریتم شبیه‌سازی متوالی مستقیم و شبیه‌سازی توامان به کار گرفته شده است. این روش جدید وارون‌سازی بر روی یک داده مصنوعی با و بدون نوفه اعمال شده است. نتایج حاصل از وارون سازی برای مقاومت صوتی وارون‌شده در هر دو حالت رضایت‌بخش بوده است. این موضوع توسط آزمون چاه‌های آزمایشی مورد تائید قرار گرفته است. همچنین یک مجموعه داده واقعی برای ارزیابی عملکرد این روش مورد استفاده قرار گرفت. نتایج حاصل از وارون‌سازی برای داده واقعی با استفاده از یک چاه آزمایشی تائید شده و توزیع فضایی مقاومت صوتی قابل‌قبول بوده است. علاوه بر آن، برای بررسی عدم قطعیت در مورد مدل‌های مقاومت صوتی وارون‌شده، واریانس این مدل‌ها مورد محاسبه و ارزیابی قرار گرفت. نتیجه این ارزیابی نشان می‌دهد که مقادیر واریانس مقاومت صوتی در مناطق دور از محل چاه افزایش می‌یابد.

کلمات کلیدی: لرزه‌شناسی، مقاومت صوتی، شبیه‌سازی متوالی مستقیم، وارون‌سازی تصادفی لرزه‌ای، الگوریتم ژنتیک.